Direct air capture of CO_2 with an Amine Resin
A molecular modeling study of the CO_2 capturing process

Buijs, Wim; de Flart, Stijn

DOI
10.1021/acs.iecr.7b02613

Publication date
2017

Document Version
Final published version

Published in
Industrial and Engineering Chemistry Research

Citation (APA)
Buijs, W., & de Flart, S. (2017). Direct air capture of CO_2 with an Amine Resin: A molecular modeling study of the CO_2 capturing process. *Industrial and Engineering Chemistry Research*, *56*(43), 12297–12304. https://doi.org/10.1021/acs.iecr.7b02613

I&EC research
Industrial & Engineering Chemistry Research

Article

Cite This: Ind. Eng. Chem. Res. 2017, 56, 12297-12304

pubs.acs.org/IECR

Direct Air Capture of CO_2 with an Amine Resin: A Molecular Modeling Study of the CO_2 Capturing Process

Wim Buijs* and Stijn de Flart

Engineering Thermodynamics, Process & Energy Department, Faculty of Mechanical, Maritime and Materials Engineering, Delft University of Technology, Leeghwaterstraat 39, 2628 CB Delft, The Netherlands

Supporting Information

ABSTRACT: Several reactions, known from other amine systems for CO_2 capture, have been proposed for Lewatit R VP OC 1065. The aim of this molecular modeling study is to elucidate the CO_2 capture process: the physisorption process prior to the CO_2-capture and the reactions. Molecular modeling yields that the resin has a structure with benzyl amine groups on alternating positions in close vicinity of each other. Based on this structure, the preferred adsorption mode of CO_2 and H_2O was established. Next, using standard Density Functional Theory two catalytic reactions responsible for the actual CO_2 capture were identified: direct amine and amine-H_2O catalyzed formation of carbamic acid. The latter is a new type of catalysis. Other reactions are unlikely. Quantitative verification of the molecular modeling results with known experimental CO_2 adsorption isotherms, applying a dual site Langmuir adsorption isotherm model, further supports all results of this molecular modeling study.

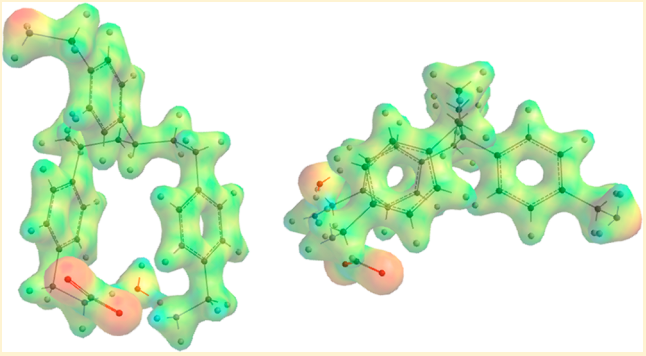

INTRODUCTION

The transition toward a more sustainable society wherein less greenhouse gases are emitted and where industrial processes become more efficient and renewable is an important topic that drives lots of research. One of the biggest challenges is to reduce the greenhouse gas emissions, especially carbon dioxide which is the main contributor to global warming.[1] Carbon dioxide emissions generally arise during the combustion of fossil fuels. Its sources can be classified as either large point sources (industrial facilities, electricity generation) or small point sources (transport, residential). Small point sources are very distributed (such as cars) and emit a lot less CO_2 compared to large point sources; however, added up they still account for more than 40% of the U.S. CO_2 emissions.[2] Limiting climate change would require substantial and sustained reductions of greenhouse gas emissions, and therefore the emissions from the small point sources cannot be ignored.

Conventional technologies are unable to address the CO_2 emissions that arise from these small point sources, which has been driving innovations in new technologies such as Direct Air Capture (DAC).[3−5] DAC aims to capture CO_2 directly from the atmosphere and utilize the captured CO_2. Therefore, it has the advantage over conventional CO_2 capture technologies that it can be used to capture CO_2 emissions unrelated to its source, allowing the technology to address CO_2 emissions arising from the smaller and distributed point sources as well. The atmosphere acts as an infrastructure for CO_2, and therefore the technology can be located anywhere. On top of this, CO_2 could be an important resource in some industrial processes such as biofuel production or water treatment.[6] By applying a DAC process at such an industrial facility it would become possible to capture and utilize the CO_2 on-site, avoiding unnecessary transport of CO_2. The literature reports many different materials and processes for CO_2 capture, of which some are capable of capturing CO_2 directly from the air.[7,8]

One rather promising group of materials for DAC is solid amine-based sorbents, which consist of a highly porous support such as fumed silica, functionalized with amine groups such as polyethylenimine (PEI).[9] Many different kinds of solid amine based sorbents have been reported in the literature for their excellent capability of separating CO_2 from the air. Most of these solid sorbents are reported to have CO_2 capacities of over 1 mol/kg under ambient conditions (400 ppm of CO_2 concentration) and can be regenerated under temperatures in the order of 100 °C.[10−13] Due to their relative low temperature of regeneration, these sorbents make up an interesting candidate for carbon capture and utilization (CCU). Processes requiring CO_2 could harvest it directly from the air, whereas the energy required for regeneration can be supplied in the form of waste heat or from renewable energy sources. This could lead to a further increase in plant efficiency as well as a sustainable source of CO_2.

Although the advantages of DAC are clear, it is not yet widely applied in industry. In order to gain a better understanding and

Received: June 26, 2017
Revised: September 13, 2017
Accepted: October 9, 2017
Published: October 9, 2017

DOI: 10.1021/acs.iecr.7b02613
Ind. Eng. Chem. Res. 2017, 56, 12297−12304

get one step closer to applying this technology in an industrial environment, this study focuses on a specific primary amine functionalized based sorbent, VP OC 1065.[14,15] Alesi et al. reported VP OC 1065 to have a stable CO_2 capacity during 18 cycles; it is almost completely regenerated at temperatures in the order of 100 °C and shows a low H_2O adsorption of 1.5 mol/kg. The full regeneration at low temperatures and the high cyclic stability make VP OC 1065 seem to be a good candidate for a DAC process. Apart from the very low CO_2 concentration of approximately 400 ppm, the concentration of water in the air (10−50.000 ppm) seems to be a very important factor too.

Despite its promising CO_2 sorption characteristics, the physical and chemical interactions of CO_2 with these materials have not been elucidated yet, contrary to the well-known aqueous amine systems wherein the formation of ammonium carbonates and carbamates has been established.

In this study, molecular modeling has been applied to gain insight into the structure of this polymeric resin, the preferred mode of adsorption of CO_2 and H_2O, and next the mechanism of the CO_2 capturing reactions. The results of the molecular simulations will be verified with available experimental CO_2 adsorption isotherms,[14] by setting up a dual site Langmuir isotherm model. Later the model will be further developed to provide important engineering parameters.

MATERIALS AND METHODS

Sorbent and Sorbent Characterization. The starting material for this molecular modeling study is Lewatit R VP OC 1065, which is an ion-exchange resin supplied by Lanxess. As the supplier reports, the resin is a polymer of *p*-vinyl benzyl amine, cross-linked with some divinylbenzene for dimensional stability. The beads have an effective size of 0.47−0.57 mm and a BET surface area of 50 $m^2\ g^{-1}$. The pore volume and average pore size are reported to be 0.27 $cm^3\ g^{-1}$ and 25 nm, respectively. Alesi and Kitchin[15] used energy-dispersive X-ray spectroscopy (EDS) to determine the composition of the resin.

Molecular Simulations. All molecular simulations were performed using Wavefunction's Spartan'16 suite.[22] Molecular mechanics (MMFF) was used to study the basic structural features of Lewatit R VP OC 1065, with and without H_2O and/or CO_2 physisorption. The results of that study were used to select candidates for chemisorption by reaction between the amine and CO_2, using quantum chemical calculations. All structures were fully optimized using density functional (DFT) B3LYP/6-31-G* starting from PM3 geometries. ωB97X-D/6 311+G(2df,2p) was used to get a more accurate estimate for the reaction energies of a model system starting from two methylamine molecules. Transition states were identified and characterized using their unique imaginary vibrational frequency or Internal Reaction Coordinate (IRC). Reaction enthalpies and activation barriers were calculated based upon total energies and enthalpy corrections. Entropy corrections were not used because of the huge simplifications of the QM-systems. Quantitative results of all calculations and all molecular (ensemble) structures are available in the Supporting Information.

Mathematical Model. As Choi et al.[9] point out, solid amine-based sorbents are expected to capture CO_2 through chemisorption, wherein the amine groups react with the CO_2 molecules. These kinds of sorbents are known to interact with water, and as Veneman et al.[14] point out for VP OC 1065 H_2O does not compete with CO_2 during adsorption but rather *enhances* the effect. The simplest way to describe noncompetitive adsorption based on several mechanisms would be through an X-site Langmuir isotherm given in the following equation

$$q^* = \frac{q_m K_i P}{1 + K_i P} \tag{1}$$

where the temperature dependency of the sorbent is described by

$$K_i = K_{0i} \exp\left(\frac{-\Delta H_{ads}}{RT}\right) \tag{2}$$

In eq 2, K_{0i} is a fitting constant, R is the universal gas constant, and ΔH_{ads} is the heat of adsorption. A correct description of the sorbent's isotherm can directly be implemented into the mass balance equation which can provide the rate of adsorption when it is matched with breakthrough experiments

$$-D_L \frac{\partial^2 c}{\partial z^2} + u\frac{\partial c}{\partial z} + \frac{\partial c}{\partial t} + \left(\frac{1-\epsilon}{\epsilon}\right)\rho_p \frac{\partial \bar{q}}{\partial t} = 0 \tag{3}$$

$$\frac{\partial \bar{q}}{\partial t} = k(q^* - \bar{q}) \tag{4}$$

where $\frac{\partial \bar{q}}{\partial t}$ is the rate of adsorption, given by the linear driving force equation (LDF), and D_L is the axial dispersion coefficient. Combined, eqs 1−4 represent a fixed bed adsorption system, assuming an isothermal trace system. These assumptions are valid for systems where the absorbable component is present at a very low concentration (negligible heat of adsorption and variation in velocity), which is the case for DAC. Eqs 1−4 are commonly used to describe a fixed bed adsorption system and can be found in the literature.[16,17] In order to solve this system of equations a correct description of the isotherm is required. A common way of obtaining this description is by performing equilibrium experiments at different temperatures and fitting this to an isotherm model. As Lu et al.[12] mentioned, theoretically any isotherm can be modeled by an *n*-site Langmuir model. In this case the experimental isotherms[14] were used to validate the molecular modeling results quantitatively. The model is available in the Supporting Information.

RESULTS AND DISCUSSION

Molecular Mechanics. The molecular composition of Lewatit R VP OC 1065, with 8.3:10.7:81.0 H:N:C on a weight basis, closely resembles the composition of a polymer based on radical polymerization of *p*-vinyl benzyl amine only. The composition of the corresponding dodecamer is 8.4:10.5:81.1 H:N:C. Therefore, the linear dodecamer was taken as a basic model for Lewatit R VP OC 1065. The 3D-structure of the dodecamer can be understood best by analyzing the geometry of the H-saturated monomer, dimer, and trimer. A conformer distribution of the monomer shows both the methylamine and ethyl group perpendicular to the aromatic ring.

Figure 1 shows the best conformation of the dimer in two representative views. The four carbon atoms form a normal zigzag chain with the two benzyl amine groups on positions 1 and 3, having a dihedral angle ($C-Ar_1,C_1,C_3,C-Ar_2$) of 107.06 degrees. The aromatic groups are in almost parallel planes, perpendicular to the alkyl chain and the amines, as in the monomer. This structural feature is preserved until conformer 4, counting up to 39.6% in the cumulative Boltzmann weights under standard conditions (ΔE-conformer 1−4 = 0.4 kJ/mol).

Figure 2 shows the 5 best conformations of the trimer of *p*-vinyl benzyl amine. The structure of the trimer is completely in

DOI: 10.1021/acs.iecr.7b02613
Ind. Eng. Chem. Res. 2017, 56, 12297−12304

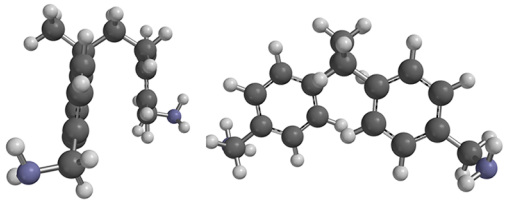

Figure 1. Best conformer of the dimer of *p*-vinyl benzyl amine.

line with the result of the conformer distribution of the dimer with respect to the orientation and position of the aromatic groups of the successive monomers. In addition the alternating aromatic groups of monomers 1 and 3 show π-stacking, and in conformers 1 and 3 H-bridging between the amino groups is shown. Conformer 1 with amine−amine H-bridging accounts for 39% of the Boltzmann weight; conformer 3 with amine−amine H-bridging accounts for 9.5%. The energy difference between conformers 1 and 5 is 5.1 kJ/mol only, roughly divided by equal steps between the conformers. Rotational barriers of the R-CH_2NH_2 groups between the conformers are <10 kJ/mol. In conclusion, the first 5 conformers account for 88% of the cumulative Boltzmann weights, and 88% is capable of amine−amine H-bridging in the trimer. Now the dodecamer can be considered as a direct continuation of the structure of the trimer. Figure 3 shows what is assumed to be the best conformer of the dodecamer. The alternating aromatic groups on 1-3, 2-4, 5-7, 6-8, 9-11, and 10-12 show π-stacking, and all amine couples are within close vicinity. Of course the same is true for the alternating aromatic and amine groups between 3 and 5, 7-9, and 4-6, 8-10. Like the trimer, the dodecamer will show approximately 88% amine−amine H-bridging.

Next the 5 best conformers of the trimer shown in Figure 3 were used to determine the preferred adsorption mode of CO_2, H_2O, and CO_2 and H_2O jointly.

Figure 4 shows the most favorable complexation of CO_2, H_2O, and CO_2 and H_2O with conformer 3 of the trimer. In all cases the complex with the lowest strain energy is obtained from conformer 3 of the trimer.

In the case of CO_2-complexation, the free electron pair of one amine group points toward the δ^+ charged C of CO_2, while a H of the second amine groups creates a hydrogen bridge to the δ^- charged O of CO_2. Conformer 1 builds an almost identical CO_2 complex, the only difference being the position of the amine group on position 2. The two complexes account for 97% in the Boltzmann weights.

In the case of H_2O-complexation, the H_2O molecule forms a hydrogen bridge with each of the amine groups. The amine−amine distance is slightly enlarged, and there is no amine−amine H-bridging anymore. This complex accounts for 99% in the Boltzmann weights. The second best complex, derived from conformer 1, shows one hydrogen bridge of H_2O to an amine and a weakened hydrogen bridge between the two amine groups. It is 14 kJ/mol higher and accounts for 0.3% only in the Boltzmann weights.

Joint CO_2 and H_2O complexation to trimer conformer 3 can be best understood as a combination of the former two single complexations. The complex accounts for >99.9% in the Boltzmann weights.

The complexes discussed above point toward two different reactions of an amine with CO_2, leading to the corresponding carbamic acid or ammonium carbamate. Details of these reactions will be discussed under quantum mechanics. The complexes of CO_2 and CO_2 and H_2O jointly with conformers 2, 4, and 5 of the trimer in a similar way point to reactions of H_2O with CO_2 to H_2CO_3 or ammonium bicarbonate. Figure 5 shows a typical example. It should be noted however that they represent <0.1% in the Boltzmann weights only.

This complex shows a hydrogen bridge of H_2O toward an amine and a hydrogen bridge of the same amine toward the δ^- charged O of CO_2, while the δ^- charge O of H_2O points toward the δ^+ charged C of CO_2.

Quantum Mechanics. Apart from the results of the molecular mechanics study on the trimer, two other aspects were considered in selecting suitable candidate reaction systems:

1. The concentration of H_2O varies largely in air.
2. Experimentally[15] it is known that Lewatit R VP OC 1065 absorbs a maximum of ~1.5 mol H_2O/kg and ~3 mol CO_2/kg.

Therefore, initially two options were considered for carbamic acid formation and one for carbonic acid formation, apart from the uncatalyzed formation of a carbamic acid from an amine and CO_2:

1. Uncatalyzed formation of carbamic acid from an amine and CO_2,
2. Amine catalyzed formation of carbamic acid,
3. Direct amine-H_2O catalyzed formation of carbamic acid,
4. Amine catalyzed formation of carbonic acid.

The structures of Figure 5a, 5c, and 6 were used to produce suitable candidate transition states. A candidate for the uncatalyzed reaction was derived from an amine-CO_2 complex directly. Initially the size of the corresponding trimers was reduced largely to

1. Methyl amine and CO_2,
2. Two methyl amines and CO_2,
3. Two methyl amines, H_2O, and CO_2, and
4. Methyl amine, H_2O, and CO_2.

The results of these calculations were used to obtain an impression of the activation barriers and reaction enthalpies. Next the structures were used as input for the analogue calculations on the full trimeric structures, except for the uncatalyzed reaction. As the uncatalyzed reaction of methyl-amine and CO_2 requires an activation barrier of 163 kJ/mol it can

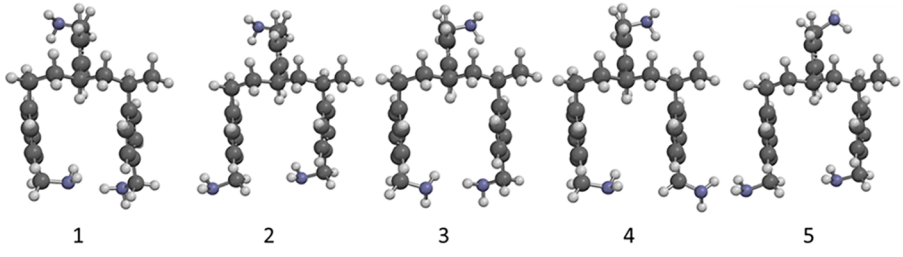

Figure 2. Best conformers (1−5) of the trimer of *p*-vinyl benzyl amine.

DOI: 10.1021/acs.iecr.7b02613
Ind. Eng. Chem. Res. 2017, 56, 12297−12304

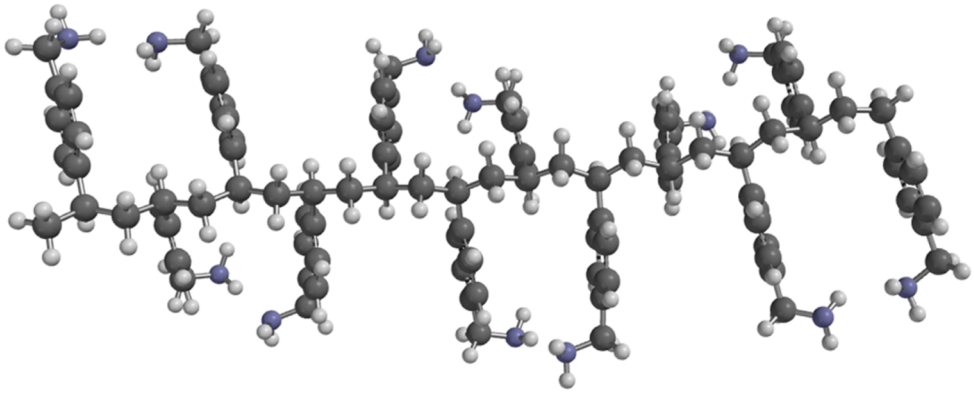

Figure 3. Best conformer of the dodecamer of *p*-vinyl benzyl amine.

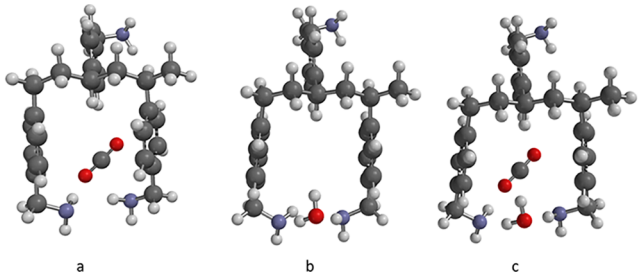

Figure 4. a: best CO_2 complex, b: best H_2O complex, and c: best CO_2 and H_2O complex with trimer conformer 3.

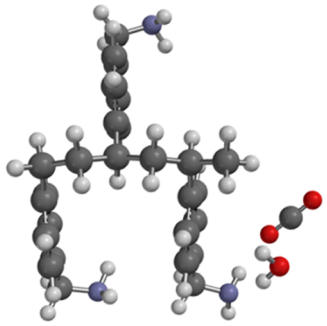

Figure 5. CO_2 and H_2O complex of trimer conformer 4.

be ruled out as a possible explanation for chemisorption of CO_2 by the resin.

Amine Catalyzed Formation of Carbamic Acid. The enthalpy of formation of the H-bridged amine-complex is about −16.5 kJ/mol in the case of methylamine and −6.7 kJ/mol only for the full trimer. The steric constraints of the trimer clearly lead to a substantial weakening of the amine−amine bridge to −6.7 kJ/mol. Complexation with CO_2 lowers the energy with ∼22 kJ/mol in all cases. The transition states shown in Figure 6 for the methyl amine and the full trimer case look very similar. Atomic distances related to the formation of the N−C bond as well as the required proton transfers are listed in the figure too. The activation barriers are 68 and 76 kJ/mol, respectively, the latter again being consistently higher as the methylamine group has to rotate out of the preferential perpendicular plane. They show simultaneous C−N bond formation, NH−N and NH−OC proton transfers to the so-called anti(carbamic acid) product. In the final products, the carbamic acids show an H-bridge to the remaining second amine. The reaction enthalpies are −75 kJ/mol and −52 kJ/mol, respectively. In the absence of any solvent no stable ammonium carbamate could be established.

Time consuming calculations using ωB97X-D/6-311+G-(2df,2p) for the methyl amine case yield almost identical results as obtained with B3LYP/6-31G* and for that reason were not applied for the full trimer. Table S1 gives an overview of all quantitative results for amine catalyzed carbamic acid formation.

Amine catalyzed formation of a carbamic acid has been investigated with DFT-calculations before. Arstad et al.[24] described already in 2007 the mono ethanolamine (MEA) catalyzed formation of the corresponding carbamic acid. In this case MEA works as a direct catalyst too. Planas et al.[18] described a very similar catalytic CO_2 capture reaction by two amines in a Metal Organic Framework (MOF). However, there is an important difference between the two reactions mentioned. Whereas Arstad et al. developed a theoretical system to describe catalysis in *aqueous* systems eventually, Planas et al. described amine catalysis in a MOF. The latter is a real system with no solvent but with very strong electrostatics, associated with the $(Mg^{2+})_2$(4,4′-dioxidobiphenyl-3,3′-dicarboxylate)$^{4-}$ of the MOF. On the other hand our Lewatit R VP OC 1065 theoretical system, the trimer of *p*-vinyl benzyl amine, resembles much more a real gas phase system than both Arstad et al. and Planas et al. In our case there is neither a solvent (H_2O) nor a strong electrostatic field present. The activation barriers obtained by Arstad et al. for an (isolated) amine catalytic system and our system are very similar: 78 (MEA) vs 76 (full trimer) kJ/mol, while the activation barrier in the MOF is much lower: 40 kJ/mol. Transition state geometries are very similar in all cases.

Direct Amine-H_2O Catalyzed Formation of Carbamic Acid. Reversible physisorption of one H_2O molecule yields −22 kJ/mol for both the methyl amine system and the full trimer. It is the result of an enthalpy gain of −55 kJ/mol and an entropy gain of +33 kJ/mol, derived from the vaporisation entropy of H_2O, 109 J/(mol K).[20] Amine-H_2O catalyzed formation of carbamic acid was described by Arstad et al.[24] in 2007 too. The difference with the former case, amine catalyzed formation of carbamic acid, is the presence of one molecule of H_2O. In the case of Arstad et al. the H_2O molecule is located on the opposite site of the second amine, which catalyzes the proton transfer from the first amine to the oxygen of the incoming CO_2 molecule. In our systems the H_2O molecule is located *between* the two benzyl amine groups as shown in Figure 5b and in more detail explained there. The transition states of amine-H_2O catalyzed carbamic acid formation are shown in Figure 7 for a methyl amine system as described by Arstad et al.[24] a methyl amine system and a full trimer system based on Figure 4b.

DOI: 10.1021/acs.iecr.7b02613
Ind. Eng. Chem. Res. 2017, 56, 12297−12304

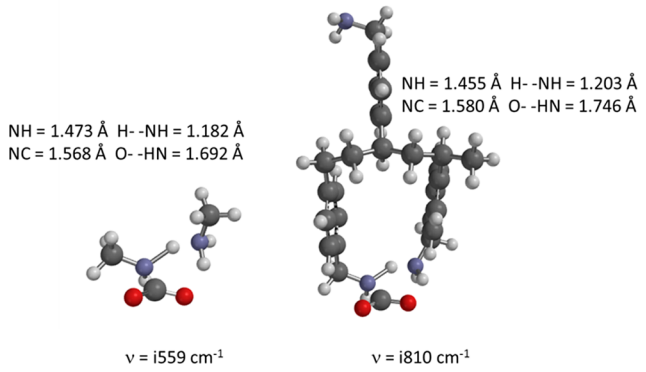

Figure 6. Transition states amine catalyzed formation of the carbamic acid:methyl amine approach and full trimer (B3LYP/6-31G*).

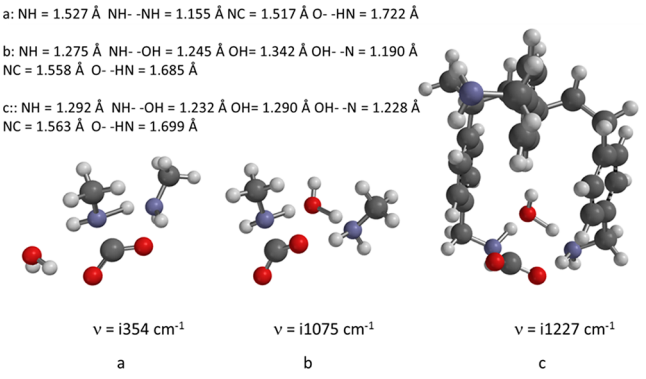

Figure 7. Transition states amine-H_2O catalyzed carbamic acid formation: a) methyl amine-H_2O according to ref 24, b) methyl amine-H_2O, and c) full trimer-H_2O (B3LYP/6-31G*).

The transition state of the methyl amine system according to Arstad et al. is entirely different from the systems derived from Figure 5b. Whereas in the system of Arstad et al. the water acts as a polar spectator, not directly involved in the proton transfers between the two amines and CO_2, in our cases the H_2O molecule is directly involved in the proton transfer from amine-H_2O-amine-CO_2. To our knowledge this type of direct amine-H_2O catalysis, with both the amine and the H_2O molecule as direct catalysts involved in proton transfers, is new. The activation barrier of the methyl amine system of Arstad et al. lies 6 kJ/mol above our systems with H_2O directly involved in the proton transfers. Therefore, this type of catalysis might well be operative in aqueous systems as well, but the reverse is not true. The corresponding methyl amine-methyl amine-H_2O complex prior to that transition state could not be established as a local minimum in B3LYP-calculations: it always transformed into the complex similar to the one shown in Figure 4b. The activation barriers of our systems are 45 kJ/mol, significantly lower as in the amine catalyzed case. This can be attributed to two effects:

1. Amine-H_2O-amine-CO_2 proton transfer is easier than amine-amine-CO_2 proton transfer only, and
2. In the full trimer there is a release of steric strain, allowing both the carbamic acid and the methylamine group in the preferred perpendicular position to the aromatic planes.

Reaction enthalpies are now −93 and −76 kJ/mol, respectively, a result of additional H-bridges in the product compared to −75 kJ/mol and −52 kJ/mol in the amine catalyzed case. Table S2 shows the results obtained from the amine-H_2O catalyzed formation of carbamic acid.

Carbamic Acid Catalyzed Formation of Carbamic Acid. The product, the H-bridged carbamic acid-amine complex, might react with a second CO_2 molecule to yield a bis-carbamic acid complex. This would require carbamic acid catalysis. This type of catalysis was described by Planas et al.[18] too. The starting point for the comparison is now the carbamic acid amine complex. Complexation with CO_2 shifts the energy to +8 kJ/mol and −3 kJ/mol, respectively. CO_2 complexation with the amine pointing to the carbon of CO_2 and a weak H-bridge of the carbamic acid to CO_2 are responsible for that effect, as is visible in the transition states shown in Figure 8 as well. As complexation of CO_2 is not favorable, this reaction is very unlikely.

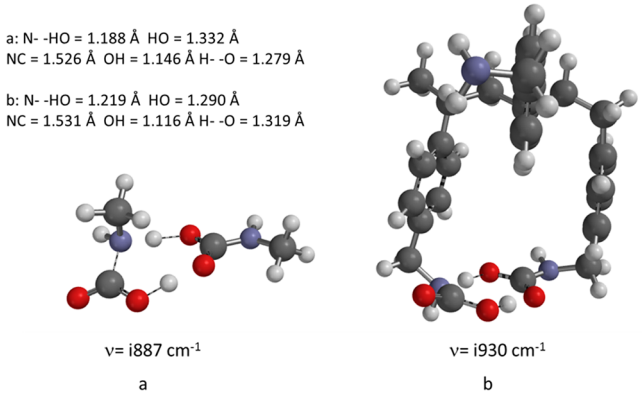

Figure 8. Transition states carbamic acid catalyzed formation of carbamic acid (B3LYP/6-31G*).

Figure 8 shows the transition states of carbamic acid catalyzed formation of (the second) carbamic acid. The transition states look very similar and show apart from NH−CO, OH−CO simultaneous proton transfers also. Activation barriers in both cases are consequently very low at 25 and 27 kJ/mol. The reaction enthalpies from the final products, the dimeric bis carbamic acids, are in both cases ∼−46 kJ/mol.

Table S3 shows all results of carbamic acid catalyzed formation of carbamic acid.

Amine Catalyzed Formation of Carbonic acid. Complexation of H_2O with a single amine does not seem to be a profitable process. The enthalpy gain and entropy loss level out. Complexation of CO_2, on the other hand with an NH−OCO hydrogen bridge and the δ^- charged O of H_2O toward the δ^+ charged C of CO_2, yields a relative energy of −21 kJ/mol, fully comparable with amine-CO_2 complexation described previously. The activation barrier is 64 kJ/mol, and the overall reaction enthalpy is −34 kJ/mol. Because the complexation of H_2O is unfavorable, this reaction is very unlikely to happen. Table S4 shows all results of methylamine catalyzed formation of carbonic acid.

FINAL DISCUSSION

Selected data of CO_2 physisorption and CO_2 capturing reactions of the full trimer are summarized in Table 1.

Direct amine-H_2O catalyzed formation of carbamic acid is clearly the most likely mechanism for CO_2-capture in Lewatit R VP OC 1065. Both CO_2 and H_2O show favorable physisorption, the activation barrier is low, and the calculated reaction enthalpy is close to the experimental value: −75.6 vs −71.0 kJ/mol for CO_2 capture in Mg_2(dobpdc).[25] Direct amine-H_2O and amine catalyzed formation of carbamic acid leads to a CO_2:RNH_2 ratio

DOI: 10.1021/acs.iecr.7b02613
Ind. Eng. Chem. Res. 2017, 56, 12297−12304

Table 1. Selected Data of CO_2 Capturing Reactions of the Full Trimer (B3LYP/6-31G*); * System: $CH_3NH_2-CO_2-CH_3NH_2$

		kJ/mol				
product	catalyst	ΔE-CO_2 compl.	ΔE-H_2O compl.	E_a-forw	E_a-back	ΔH
RNHCOOH H_2NR	RNH_2-H_2O	−19.1	−22.4	44.3	42.2	−75.6
	RNH_2	−19.8		75.9	82.3	−51.6
2 RNHCOOH	RNHCOOH	−2.9		27.4	12.4	−45.0
H_2CO_3-H_2NR*	RNH_2	−21.0	1.7	64.4	64.7	−33.6

= 1:2. Combined with the earlier mentioned ~(88%*99%=)87% presence of conformers capable of amine−amine H-bridging, and the resin's molecular composition of 7.50 mol RNH_2/kg, the here presented description leads to an overall value of ~3.2 mol CO_2/kg, as the upper limit of CO_2 capture. This is quite close to the reported maximum value of 3.0 mol CO_2/kg resin under a full CO_2 atmosphere.[15]

However, as the apolar resin absorbs only 1.5 mol H_2O/kg, while 3 mol CO_2/kg can be captured,[15] an additional catalytic reaction is needed. The second best option is amine catalyzed formation of carbamic acid. CO_2 shows favorable physisorption, the activation barrier is moderately high with 75.9 kJ/mol, and the calculated reaction enthalpy −51.6 kJ/mol.

Carbamic acid catalyzed formation of carbamic acid is unlikely, as the CO_2-complex is weak (−2,9 kJ/mol), and the reverse reaction is even faster. Furthermore the process leads to a CO_2:RNH_2 ratio = 2:2. Finally amine catalyzed formation of carbonic acid is unlikely as the single amine-H_2O complex is very weak (−1.7 kJ/mol), and the reaction enthalpy is too low (−33.6 kJ/mol).

Mathematical Model for CO_2-Chemisorption. The reaction enthalpies of amine-H_2O and amine catalyzed formation of carbamic acid were used to describe the temperature dependency of the CO_2 capacity of Lewatit R VP OC 1065 in a packed bed column. Values for K_{01} and K_{02} were obtained by fitting this model to experimental data from Veneman et al.,[14] at a temperature of 303 K. The experimental data were extracted by making use of a WebPlotDigitizer tool.[19] The X-site Langmuir isotherm was reduced to a *dual site* model in order to describe the sorbent's CO_2 capacity:

$$q^* = \frac{q_{m1}K_1P}{1 + K_1P} + \frac{q_{m2}K_2P}{1 + K_2P}$$

$$K_i = K_{0i}\exp\left(\frac{-\Delta H_{ads,i}}{RT}\right)$$

It should be noted that a single site Langmuir isotherm model cannot reproduce the experimental data adequately, while a triple site model does not lead to any improvement. Table 2 shows the input parameters at 303 K. Using the data shown in Table 2, the equilibrium capacities can be calculated for each temperature according to the dual site model. Figures 9 and 10 show the results of these calculations compared to experimental data as well as at conditions relevant for direct air capture.

Table 2. Input Parameters for the Dual Site Model That Were Obtained from Curve Fitting at 303 K

parameter	value	source
q_{m1} (mol/kg)	1.94	curve fitting
q_{m2} (mol/kg)	1.06	curve fitting
K_1 (Pa^{-1})	0.01201	curve fitting
K_2 (Pa^{-1})	0.0001444	curve fitting
ΔH_1 (kJ/mol)	−75.6	Table 1 line 1
ΔH_2 (kJ/mol)	−51.6	Table 1 line 2

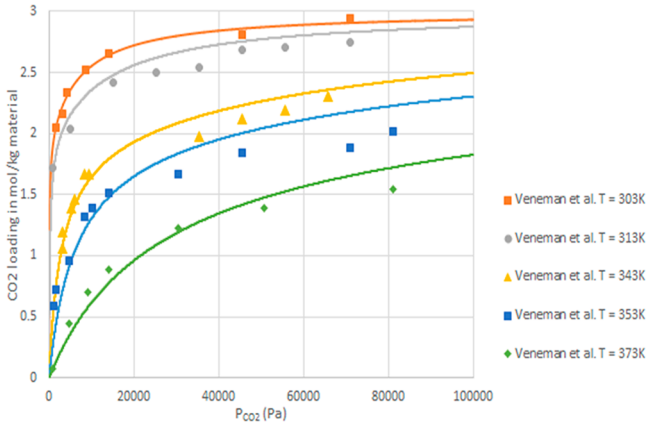

Figure 9. CO_2 adsorption isotherms for VP OC 1065 at 303 K, 313 K, 343 K, 353 K, and 373 K. Solid lines represent the CO_2 capacity, calculated according to the dual site Langmuir model. Experimental data were taken from Veneman et al.[14]

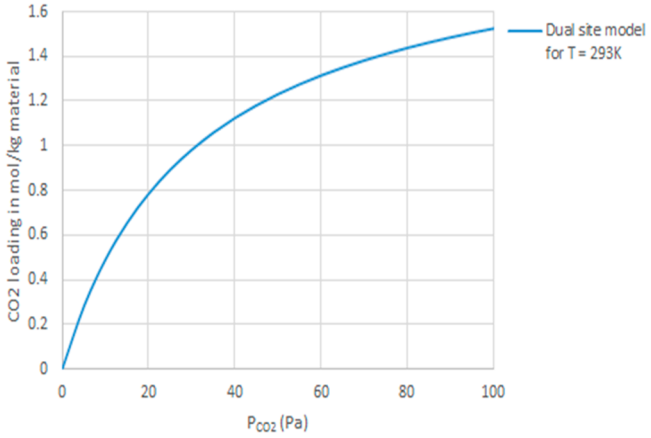

Figure 10. Calculated CO_2 capacity at direct air capture conditions for VP OC 1065.

From Figure 9 it can be seen that the dual site model predicts the CO_2 capacity at different temperatures quite well, when compared to the experimental values. The maximum capacity, at 303 K, resulting from the initial curve fitting, is (1.94 + 1.06) = 3.0 mol CO_2/kg. The predicted curves are slightly too high with increasing CO_2 pressure and temperature. This might be due to the lack of any limiting dynamics in the model (mass transfer limitation,[21] chemical kinetics) or deactivation by CO_2. Very recently Yu et al. reported degradation of Lewatit R VP OC 1065 in concentrated dry CO_2 at $T > 120$ °C.[23] A possible deactivation route will be reported separately soon.

DOI: 10.1021/acs.iecr.7b02613
Ind. Eng. Chem. Res. 2017, 56, 12297−12304

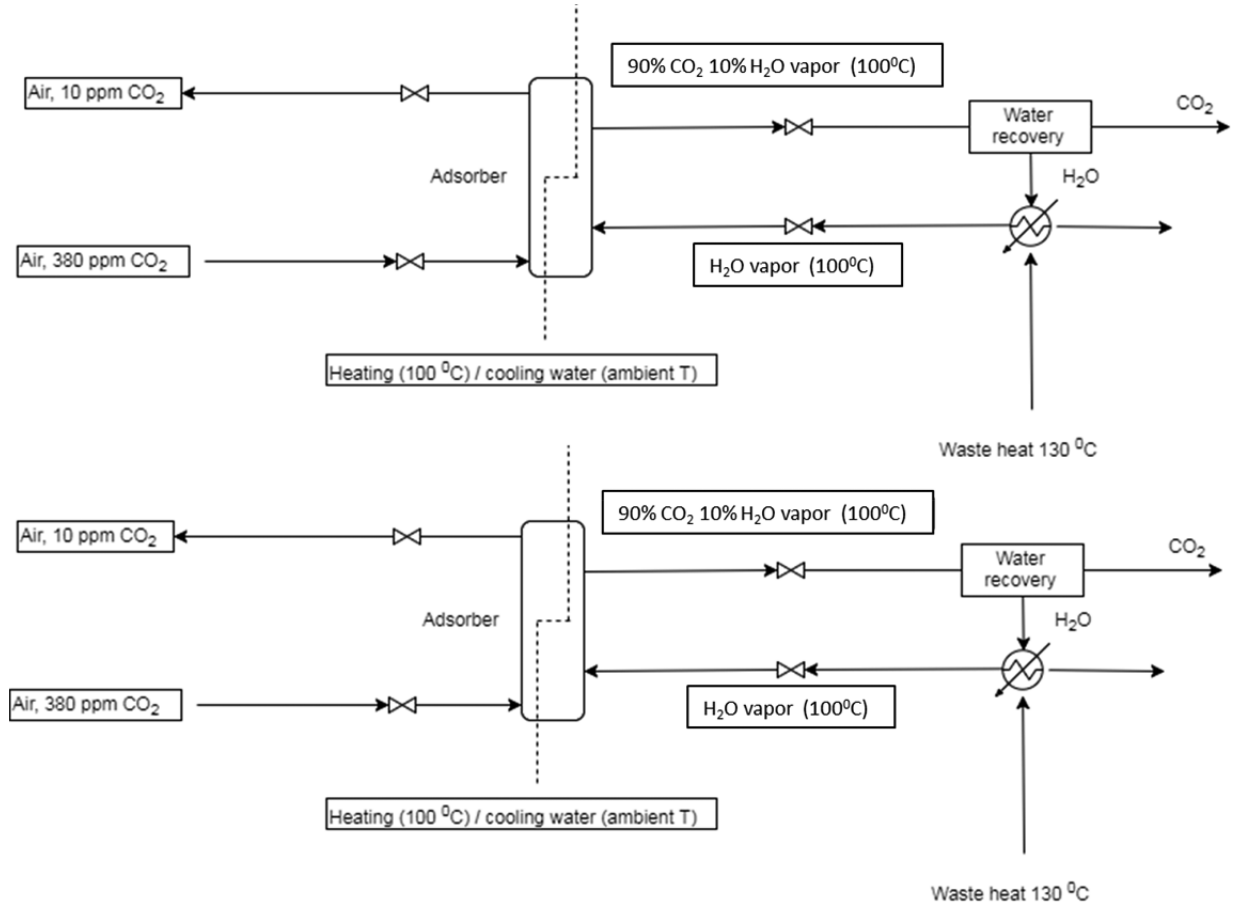

Figure 11. A simple DAC process using two fixed bed columns.

From Figure 10 it is clear that at 400 ppm of CO_2 and T = 293 K, the capacity of the resin is still ~1.1 mol CO_2/kg which is crucial for application in a DAC process.

DAC Process. For a DAC process using Lewatit R VP OC 1065 it is also important to realize that the capture of 1 kg CO_2 requires a flow of ~1400 m^3 of air through ~23 kg of resin. This will prohibit the use of the resin as a permanent storage material. It should be considered as a temporary storage material or, expressed more accurately, as an effective CO_2 concentrator. Figure 11 shows the most simple fully continuous process, with two fixed bed columns, one operating in adsorption mode and one in desorption mode.

In adsorption mode one fixed bed column is fed with air, containing ~380 ppm of CO_2 at ambient outside temperature (298 K). The outlet stream is arbitrarily set at 10 ppm of CO_2 (97% conversion). The temperature in the column is actively maintained by using cooling water. The second column is operated at the same time in desorption mode at 100 °C by heating up the cooling water to that temperature using "waste" heat or geothermal energy to avoid unwanted condensation of H_2O. A small H_2O vapor stream at 100 °C is led through to produce a concentrated (90%) CO_2 stream. The H_2O vapor is required to avoid deactivation of the resin by dry CO_2 as reported by Yu et al.[23] It should be noted that this way of operating the process is only possible because of the low amount of H_2O adsorption on the resin. This allows on one side the herein reported direct amine-H_2O catalysis, while on the other side also desorption of a concentrated CO_2 stream with a small H_2O vapor stream is possible. If a material would be used showing a much higher H_2O adsorption, the overall energetics of the process would be dominated by the adsorption and desorption of water. In a process using a material with the H_2O adsorption of Lewatit R VP OC 1065 the overall energetics might be limited to the required entropy of (ideal) gas separation, the heat of reaction, and the energy to heat up the resin to the desired desorption temperature (100 °C). In this fully continuous process, using at least two columns, the heat of reaction, released in adsorption mode, partly could be reused for preheating the water stream in desorption mode.

Finally it should be noted that apart from its suitability for a DAC-process, the resin also can be applied for point sources of CO_2. The same properties that make it particularly useful for a DAC process (high CO_2 capacity, low H_2O capacity, low desorption temperature) are important for such processes as well.

CONCLUSIONS

1. A molecular mechanics study on the structure of Lewatit R VP OC 1065 yields that the resin has an ordered structure wherein alternating amine groups are within close vicinity to enable specific catalytic CO_2 capturing reactions.
2. Two catalytic reactions are responsible for CO_2 capture on Lewatit R VP OC 1065: direct amine-H_2O and amine catalyzed formation of carbamic acid.
3. Direct amine-H_2O catalysis is a new catalytic reaction.
4. The formation of ammonium carbonate on the resin is very unlikely.

DOI: 10.1021/acs.iecr.7b02613
Ind. Eng. Chem. Res. 2017, 56, 12297−12304

5. Carbamic acid catalyzed formation of carbamic acid is very unlikely.
6. The use of ωB97X-D/6-311+G(2df,2p) yields almost identical results as obtained with B3LYP/6-31G* and seems of limited added value.
7. Quantitative verification of the molecular modeling results with known experimental CO_2 adsorption isotherms, applying a dual site Langmuir isotherm model, further supports all results of this molecular modeling study.
8. This study and the references herein cited on computational chemistry are an ongoing demonstration of the fact that molecular modeling is capable of solving a variety of thermodynamic and engineering problems in very specific cases while using a general applicable approach.

■ ASSOCIATED CONTENT

Supporting Information

The Supporting Information is available free of charge on the ACS Publications website at DOI: 10.1021/acs.iecr.7b02613.

Tables S1−S4 (PDF)

Molecular modeling data, Lewatit isotherm model, and all molecular structures (ZIP)

■ AUTHOR INFORMATION

Corresponding Author

*E-mail: w.buijs@tudelft.nl.

ORCID

Wim Buijs: 0000-0003-3273-5063

Notes

The authors declare no competing financial interest.

■ ACKNOWLEDGMENTS

This work was supported by EBN. Their cooperation is hereby gratefully acknowledged.

■ REFERENCES

(1) IPCC, Summary for Policymakers. In *Climate Change 2013: The Physical Science Basis. Contribution of Working Group I to the Fifth Assessment Report of the Intergovernmental Panel on Climate Change*; Stocker, T. F., Qin, D., Plattner, G.-K., Tignor, M., Allen, S. K., Boschung, J., Nauels, A., Xia, Y., Bex, V., Midgley, P. M., Eds.; Cambridge University Press: Cambridge, United Kingdom and New York, NY, USA, 2013.

(2) EPA United States Environmental Protection Agency. U.S. Carbon Dioxide emissions, by source. https://www.epa.gov/ghgemissions/overview-greenhouse-gases#carbon-dioxide (accessed 2016-01-04).

(3) Keith, D. W.; Ha-Duong, M.; Stolaroff, J. K. Climate strategy with CO_2 capture from the air. *Clim. Change* **2006**, *74* (1−3), 17−45.

(4) Stolaroff, J. K. *Capturing CO_2 from ambient air: a feasibility assessment*, Ph.D. Thesis, Carnegie Mellon University: Pittsburgh, PA, 2006.

(5) Lackner, K. S.; Grimes, P.; Ziock, H.-J. Carbon dioxide extraction from air: is it an option? 24th Annual Technical Conference on Coal Utilization & Fuel Systems, 1999.

(6) Aresta, M. *Carbon dioxide as chemical feedstock*; John Wiley & Sons: 2010; DOI: 10.1002/9783527629916.

(7) Wang, J.; Huang, L.; Yang, R.; Zhang, Z.; Wu, J.; Gao, Y.; Wang, Q.; O'Hare, D.; Zhong, Z. Recent advances in solid sorbents for CO_2 capture and new development trends. *Energy Environ. Sci.* **2014**, *7* (11), 3478.

(8) Wang, Q.; Luo, J.; Zhong, Z.; Borgna, A. CO_2 capture by solid adsorbents and their applications: current status and new trends. *Energy Environ. Sci.* **2011**, *4* (1), 42.

(9) Choi, S.; Drese, J. H.; Jones, C. W. Adsorbent materials for carbon dioxide capture from large anthropogenic point sources. *ChemSusChem* **2009**, *2* (9), 796.

(10) Chen, Z.; Deng, S.; Wei, H.; Wang, B.; Huang, J.; Yu, G. Polyethylenimine-impregnated resin for high CO_2 adsorption: an efficient adsorbent for CO_2 capture from simulated flue gas and ambient air. *ACS Appl. Mater. Interfaces* **2013**, *5* (15), 6937.

(11) Belmabkhout, Y.; Serna-Guerrero, R.; Sayari, A. Adsorption of CO_2-containing gas mixtures over amine-bearing pore-expanded mcm-41 silica: application for gas purification. *Ind. Eng. Chem. Res.* **2010**, *49* (1), 359.

(12) Lu, W.; Sculley, J. P.; Yuan, D.; Krishna, R.; Zhou, H.-C. Carbon dioxide capture from air using amine-grafted porous polymer networks. *J. Phys. Chem. C* **2013**, *117* (8), 4057.

(13) Chaikittisilp, W.; Khunsupat, R.; Chen, T. T.; Jones, C. W. Poly (allyamine)-mesoporous silica composite materials for CO_2 capture from simulated flue gas or ambient air. *Ind. Eng. Chem. Res.* **2011**, *50* (24), 14203.

(14) Veneman, R.; Zhao, W.; Li, Z.; Cai, N.; Brilman, D. W. F. Adsorption of CO_2 and H_2O on supported amine sorbents. *Energy Procedia* **2014**, *63*, 2336.

(15) Alesi, W. R., Jr; Kitchin, J. R. Evaluation of a primary amine-functionalized ion-exchange resin for CO_2 capture. *Ind. Eng. Chem. Res.* **2012**, *51* (19), 6907.

(16) Ruthven, D. M. *Principles of adsorption and adsorption processes*; John Wiley & Sons: 1984.

(17) Shafeeyan, M. S.; Daud, W. M. A. W.; Shamiri, A. A review of mathematical modeling of fixed-bed columns for carbon dioxide adsorption. *Chem. Eng. Res. Des.* **2014**, *92* (5), 961.

(18) Planas, N.; Dzubak, A. L.; Poloni, R.; Lin, L.-C.; McManus, A.; McDonald, T. M.; Neaton, J. B.; Long, J. R.; Smit, B.; Gagliardi, L. The Mechanism of Carbon Dioxide Adsorption in an Alkylamine-Functionalized Metal−Organic Framework. *J. Am. Chem. Soc.* **2013**, *135*, 7402.

(19) Rohatgi, A. WebPlotDigitizer. http://arohatgi.info/WebPlotDigitizer/ (accessed 2016-02-25).

(20) A list of thermodynamical properties of water can be found at http://www1.lsbu.ac.uk/water/water_properties.html (accessed 2017-10-13).

(21) Goeppert, A.; Zhang, H.; Czaun, M.; May, R. B.; Prakash, S.; Olah, G. A.; Narayanan, S. R. Easily Regenerable Solid Adsorbents Based on Polyamines for Carbon Dioxide Capture from the Air. *ChemSusChem* **2014**, *7*, 1386.

(22) Wavefunction Inc., 18401 Von Karman Avenue, Suite 370, Irvine, CA 92612, U.S.A. www.wavefun.com (accessed 2017-10-13).

(23) Yu, Q.; de la Delgado, J.; Veneman, R.; Brilman, D. W. F. Stability of a Benzyl Amine Based CO_2 Capture Adsorbent in View of Regeneration Strategies. *Ind. Eng. Chem. Res.* **2017**, *56*, 3259.

(24) Arstad, B.; Blom, R.; Swang, O. CO_2 Absorption in Aqueous Solutions of Alkanolamines: Mechanistic Insight from Quantum Chemical Calculations. *J. Phys. Chem. A* **2007**, *111*, 1222.

(25) McDonald, T. M.; Lee, W. R.; Mason, J. A.; Wiers, B. M.; Hong, C. S.; Long, J. R. Capture of Carbon Dioxide from Air and Flue Gas in the Alkylamine- Appended Metal−Organic Framework mmen-Mg_2(dobpdc) J. *J. Am. Chem. Soc.* **2012**, *134*, 7056.

DOI: 10.1021/acs.iecr.7b02613
Ind. Eng. Chem. Res. 2017, 56, 12297−12304